Investigation of the Protective Armours for Gamma Rays and Fast Neutrons Parameters

Zaid Muzher Nuri[1], Asmaa Ahmed Aziz[1], Sabah Mahmoud Aman Allah[2]

[1]Department of Physics – College of Education for Pure Sciences – University of Tikrit – Salah AL-Din - Iraq.
[2]Department of Physics – College of Education for Pure Sciences – University of Kirkuk – Kirkuk - Iraq.
Email: JA230033pep@st.tu.edu.iq

In the present research, several materials that can be used as shields against ionizing radiation (gamma and neutrons) were studied. The metallic compounds shown in Table (1) were used to test them in shielding against γ rays. The μ_t was found using NIST-XCOM within the energy range (59.53-10^9) keV, and it became clear that there was a difference in their attenuation values, and the results showed that the best of these compounds in the attenuation of γ rays were (Fe_3 O_4) because it contains a large percentage of iron with a relatively large Z. Five glass samples shown in Table (2) were also studied to evaluate their ability to attenuate fast neutrons, using the SAZ code written in the Python programming language. The most important of these parameters is the effective removal cross-section for fast neutron Σ_R. The results showed that the best sample was (S5), as it has the biggest value for Σ_R. It also turns out that the best sample from the group of samples studied in Table (3) is Steel Alloy because it has the best neutron attenuation parameters.

Keywords: Atomic effective number, attenuation of neutrons, gamma, cross-section, electronic density, half, tenth layer, mass attenuation coefficients, NIST-XCOM, SAZ code.

1. Introduction

Nuclear technology is used in multiple fields such as industry, medicine, agriculture, etc. So the human needs to protect himself and his environment from the dangers of resulting ionizing radiation, such as gamma rays and neutrons [1]. By using radiation shields, the risks of these rays can be reduced. There are many types of shields that are different depending on the type of radiation, its energy, and the type of shielding material. Shielding against neutrons must be made of materials with small atomic numbers, especially materials

containing hydrogen in their composition [2], while shields against gamma rays need materials with large atomic numbers [3]. The attenuation parameters of γ-rays and neutrons have been studied with different methods and materials, as in [4-17].

Calculations

I- Gamma-ray interactions with matter

Gamma rays interact with matter in different ways, the most important of which are the following:

1- Photoelectric phenomenon: It occurs at low energies, and it is a process through which a photon expels one of the orbital electrons from the atom, which are then called photoelectrons [18].
2- Compton scattering: It occurs at medium energies. It represents the scattering of a photon by a stationary and free electron. Some of the photon's energy is transferred to the electron, changing its energy and direction of movement. Electron density is a determining factor for the macroscopic Compton scattering cross-section [19].
3- Pair production: It occurs in the nuclear field, and it is a process in which the photon loses all its energy to its empty surroundings, producing an electron-positron pair. The photon must have an initial energy E greater than the masses of the electron and positron together $1.022\,\frac{\mathrm{MeV}}{c^2}$ [18].
4- Triple Production: It occurs in the atomic field, and for it to take place, it requires $E_\gamma = 2.044$ MeV, and it occurs through the fall of a γ photon on the orbiting electron to be expelled, and the photon turns into an electron and a positron, thus producing three particles: a pair of electrons and a positron [20].

Mass attenuation coefficient of gamma rays $\mu_t\left(\frac{cm^2}{g}\right)$

This coefficient represents a measure of the probability of a γ photon interacting with matter, it's given by [21]:

$$\mu_t = \frac{\mu}{\rho} \dots\dots\dots\dots (1)$$

Whereas $\mu(cm^{-1})$ and $\rho\left(\frac{g}{cm^3}\right)$ are the linear attenuation coefficient and the material density, respectively. For mixtures and compounds, it's calculated from the relationship [22]:

$$\mu_t = \sum_i w_i(\mu_t)_i \dots\dots\dots\dots\dots (2)$$

Whereas $w_i = \frac{n_i A_i}{\sum_i n_i A_i}$: the weight fraction of the elements in the compound or mixture, as n_i and A_i represent the atomic weight and number of atoms of the i^{th} element, respectively [23]. The total molecular cross-section $\sigma_{t,m}$ can be calculated from the relationship [21]:

$$\sigma_{t,m} = \mu_t \frac{M}{N_A} \dots\dots\dots (3)$$

Where M: molecular weight, and N_A: Avogadro's number [24]. The total atomic cross-

section $\sigma_{t,a}$ can be calculated from the relationship [25]:

$$\sigma_{t,a} = \frac{\sigma_{t,m}}{\sum_i n_i} \dots\dots\dots (4)$$

The total electronic cross section $\sigma_{t,e}$ is calculated from the relation [26]:

$$\sigma_{t,e} = \frac{1}{N_A} \sum_i f_i \frac{A_i}{Z_i} (\mu_t)_i \dots\dots\dots (5)$$

Whereas $f_i = \frac{n_i}{\sum_i n_i}$: the fractional abundance of atoms of the i^{th} element in the compound, and Z_i: it's atomic number [27]. The effective atomic number (Z_{eff}), which represents the ratio between the total atomic and electronic cross-sections, can be given by [21]:

$$Z_{eff} = \frac{\sigma_{t,a}}{\sigma_{t,e}} \dots\dots\dots (6)$$

The electronic density (N_e) represents the number of interacting electrons per unit mass of the attenuated material, and it's given by [27] :

$$N_e = \frac{\mu_t}{\sigma_{t,e}} = N_A \frac{Z_{eff}}{\sum_i f_i A_i} \dots\dots\dots\dots (7)$$

The mean free path (λ) represents the average distance that the rays travel inside the attenuating material without interacting with it, and is given by the equation [28]:

$$\lambda\ (cm) = \frac{1}{\Sigma_R} \dots\dots\dots\dots (8)$$

The half value layer (HVL) represents the required thickness of the attenuation material at which the intensity of the rays falling on the material decreases to half its original intensity, and is given by the relationship [9]:

$$HVL(cm) = \frac{\ln(2)}{\Sigma_R} \dots\dots\dots\dots (9)$$

The tenth value layer (TVL) represents the thickness of the attenuation material required to reduce the intensity of the rays to one-tenth of its original intensity, and it's given by [9]:

$$TVL(cm) = \frac{\ln(10)}{\Sigma_R} \dots\dots\dots\dots (10)$$

A number of eco-friendly metallic compounds shown in table (1) were used in studying the attenuation of γ-rays. One of the important factors in choosing a shielding material against γ-rays is that it should have a large Z and a high ρ, and be highly attenuating, in addition to its thickness. It is also preferable that it be environmentally friendly. It does not cause harm to the environment when used, disposed of, or recycled, and it is easy to remove heat from it, in addition to its good resistance to radiation damage, in addition to its low cost of obtaining it, and its advantage of structural durability [19].

Table (1): the compounds used in studying gamma ray attenuation, with their densities.

Composites	ρ $\left(\frac{g}{cm^3}\right)$
Fe_2O_3	5.27
Fe_3O_4	5.20
$FeTiO_3$	4.79
TiO_2	4.25

II- Neutrons interaction with matter

Due to the large range of neutron energies; the process of shielding against neutrons is very complex. Among the most important interactions of neutrons with matter are the following [29]:

1- Elastic scattering: When a neutron collides with the nucleus in a collision similar to the collision of billiard balls and bounces off of it, it loses a very small portion of its initial energy to be transferred to the nucleus in the form of kinetic energy [30].
2- Inelastic scattering: The colliding neutron transfers some of its energy to the scattering nucleus, causing it to be excited. Then the nucleus releases γ rays by rearranging the energy levels to stabilize them [29].
3- Neutron capture: The nucleus captures neutrons, which excites them. To stabilize them, they emit a γ particle or photon, which is a factor in determining the design of shields. A material with a large Z is often incorporated to absorb the resulting γ rays [29].

Effective removal cross section of neutrons $\boldsymbol{\Sigma_R}\ \left(\boldsymbol{cm^{-1}}\right)$

The $\boldsymbol{\Sigma_R}$ of fast neutrons describes the probability of the fast neutron that undergoes the first interaction from the group of penetrating uncollision neutrons[30]. It can be calculated for chemical compounds or mixtures from the equation [31]:

$$\boldsymbol{\Sigma_R = \sum_i \rho_i \left(\frac{\Sigma_R}{\rho}\right)_i} \ldots\ldots\ldots\ldots (\mathbf{11})$$

Where $\boldsymbol{\rho_i}\left(\frac{g}{cm^3}\right)$: the partial density, and $\left(\frac{\Sigma_R}{\rho}\right)_i\left(\frac{cm^2}{g}\right)$: the removal mass cross-section of the $\boldsymbol{i^{th}}$ element [2], and can be calculated through semi-empirical equations based on Z and A, like James Wood's semi-empirical equation that given by form [32]:

$$\boldsymbol{\frac{\Sigma_R}{\rho} = 0.206 A^{-\frac{1}{3}} \cdot Z^{-0.294}} \ldots\ldots (\mathbf{12})$$

Whereas Z, A are the atomic and mass numbers, respectively. $\frac{\Sigma_R}{\rho}$ can also be calculated from Zoller's two semi-empirical equations, which are given by form [33]:

$$\boldsymbol{\frac{\Sigma_R}{\rho} = 0.19 Z^{-0.743}} \quad , \quad \boldsymbol{Z \leq 8} \ldots\ldots (\mathbf{13})$$

$$\boldsymbol{\frac{\Sigma_R}{\rho} = 0.125 Z^{-0.565}} \quad , \quad \boldsymbol{Z > 8} \ldots\ldots (\mathbf{14})$$

To calculate (TVL, HVL, $\boldsymbol{\lambda}$) for neutrons, the same equations (10,9,8) can be used,

respectively.

Results & Discussion

Gamma-ray attenuation parameters were calculated using the NIST-XCOM database on the Internet website.

I- Gamma ray attenuation - calculation

Figure (1) shows the mass attenuation coefficient $\boldsymbol{\mu_t}$ for several eco-friendly compounds shown in Table (3), and the results showed that $\boldsymbol{\mu_t}$ decreases rapidly with increasing incident photon energy. The compound ($\boldsymbol{Fe_3O_4}$) has the highest value of $\boldsymbol{\mu_t}$, and the lowest value for the compound ($\boldsymbol{TiO_2}$) at the same energy, and this can be attributed to the large $\boldsymbol{\sigma_{pe}}$ of gamma-ray attenuation, which is proportional to $\frac{\boldsymbol{Z^{4.6}}}{\boldsymbol{E^{3.5}}}$, as the photoelectric phenomenon is dominant [34]. Compton scattering dominates at intermediate energies, where $\boldsymbol{\sigma_{cs}}$ is proportional to $\frac{\boldsymbol{Z}}{\boldsymbol{E}}$ [35]. $\boldsymbol{\mu_t}$ increases slightly, as in the side view of Figure (1), due to the proportionality of $\boldsymbol{\sigma_{pp}}$ to $\boldsymbol{Z^2}$, where the pair production interaction is dominant and then stabilizes at high energies $\boldsymbol{E \geq 100\ MeV}$ [36,37].

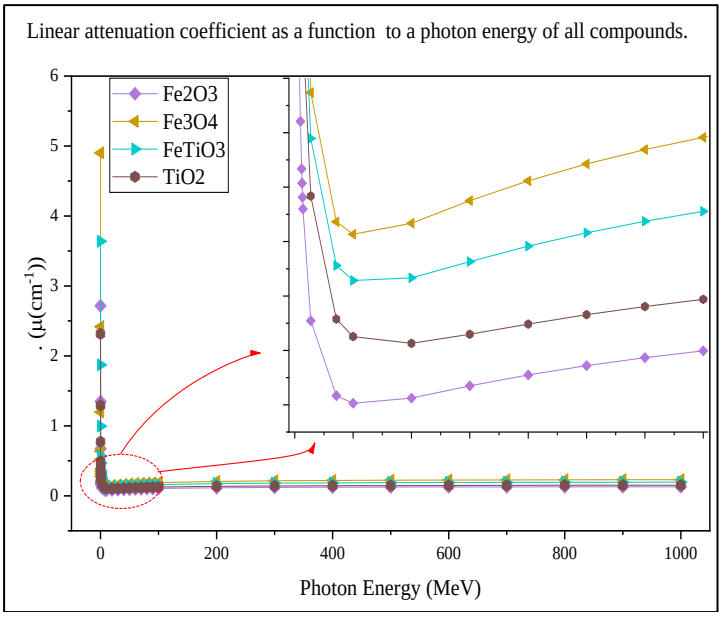

Fig (1): Mass attenuation coefficient versus photon energy.

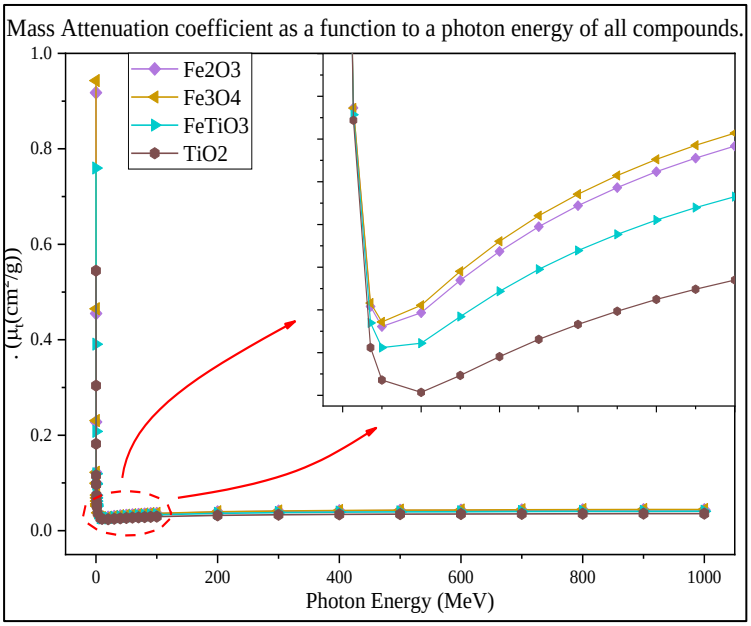

Fig (2): Linear attenuation coefficient versus photon energy.

Figure (2) shows the linear attenuation coefficient $\boldsymbol{\mu}$, as $\boldsymbol{\mu}$ decreases with increasing energy of the incident photon and then increases slightly at high energies. The biggest value was for the compound ($\boldsymbol{Fe_3O_4}$) and the minimum value was for the compound ($\boldsymbol{TiO_2}$) at the same energy. The big value to $\boldsymbol{\mu}$ for ($\boldsymbol{Fe_3O_4}$) due to its density; $\boldsymbol{\mu}$ depends on the density of the substance, as well as the fact that it contains Fe with a high Z compared to other compounds.

Figure (3) shows the total molecular cross-section $\boldsymbol{\sigma_{t,m}}$, as it is high at small photon energies, and gradually decreases with increasing energy. The largest value of $\boldsymbol{\sigma_{t,m}}$ is for the compound ($\boldsymbol{Fe_3O_4}$), as $\boldsymbol{\sigma_{t,m}}$ is directly proportional to $\boldsymbol{\mu_t}$ due to the big value of $\boldsymbol{\sigma_{pe}}$ at the minimum energy, and the compound ($\boldsymbol{TiO_2}$) has a least value because it's less dense and contains lighter elements.

Figure (4) shows the total atomic cross-section $\boldsymbol{\sigma_{t,a}}$, which is large and then begins to decrease rapidly to a certain extent, then begins to increase slightly with increasing photon energy when the phenomenon of pair production is most influential. The maximum value of $\boldsymbol{\sigma_{t,a}}$ was for the compound ($\boldsymbol{Fe_3O_4}$) and the lowest value for $\boldsymbol{\sigma_{t,a}}$ at the same energy was for the compound ($\boldsymbol{TiO_2}$), due to the presence of atoms with a small Z in it. We also note its stability at high energies.

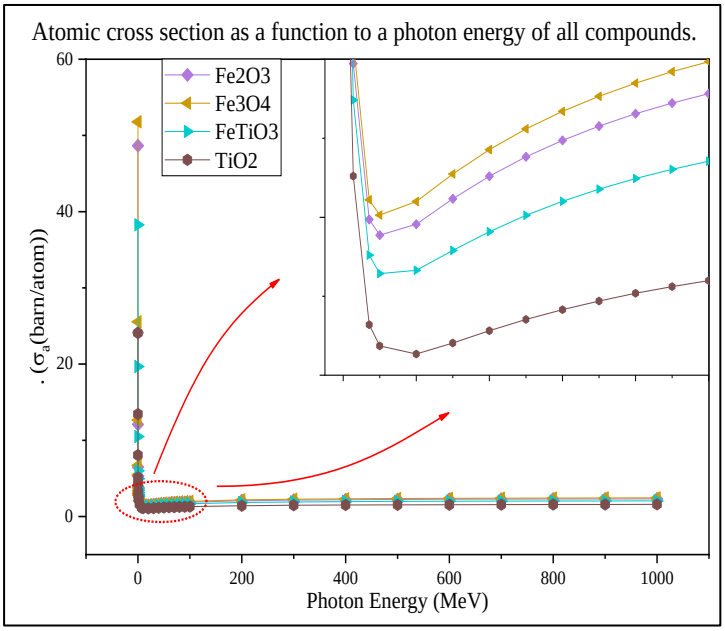

Fig (3): Total molecular cross-section versus photon energy.

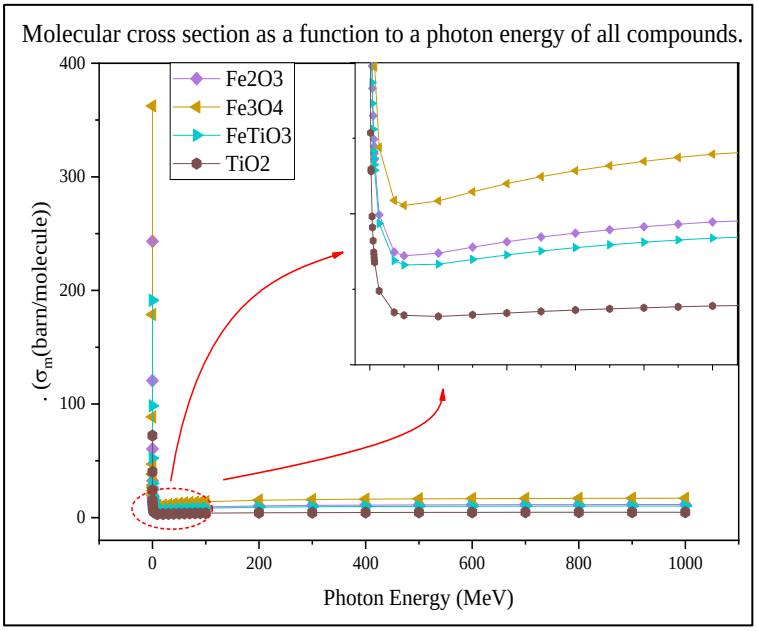

Fig (4): Total atomic cross-section versus photon energy.

Figure (5) shows the total electronic cross-section $\boldsymbol{\sigma_{t,e}}$, and it starts with a large values at small photon energies, then decreases rapidly to a certain extent, then its amount increases slightly. The biggest value of $\boldsymbol{\sigma_{t,e}}$ was for the compound ($\boldsymbol{Fe_3O_4}$), and the least value for $\boldsymbol{\sigma_{t,e}}$ was for the compound ($\boldsymbol{TiO_2}$) at the same energy, and the explanation for this is due to the difference in the number of electrons that the photon encounters in both compounds.

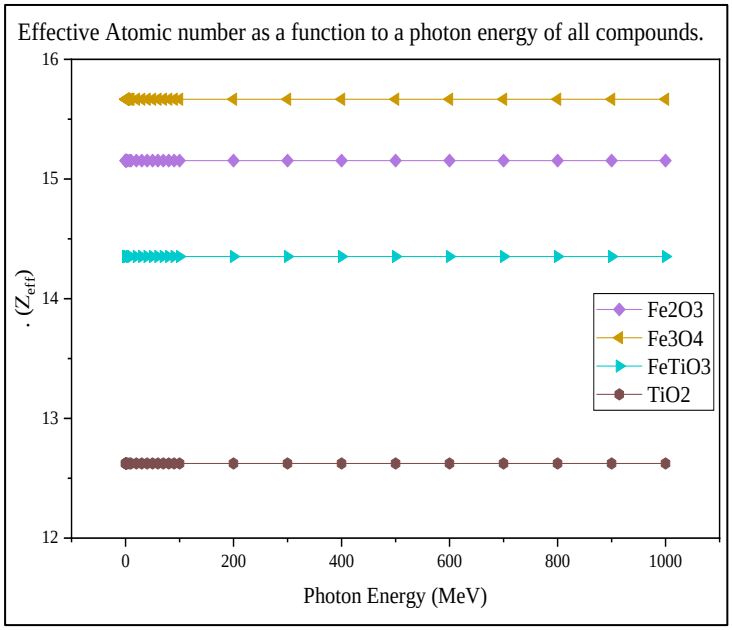

Fig (5): Total electronic cross section versus photon energy.

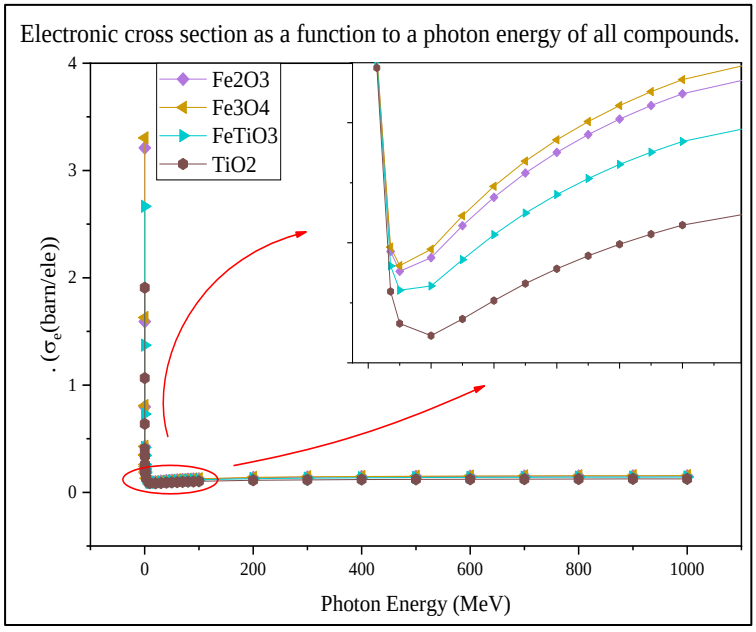

Fig (6): Effective atomic number versus photon energy.

Figure (6) shows the effective atomic number $\boldsymbol{Z_{eff}}$, and we note that it has a constant value for the photon energies studied, as its values are equal to (12.623, 14.353, 15.666, 15.154) for the compounds ($\boldsymbol{TiO_2, FeTiO_3, Fe_3O_4, Fe_2O_3}$) respectively, and its amount changes with the chemical composition of the compound. The highest value is for ($\boldsymbol{Fe_3O_4}$), due to it containing the biggest number of electrons, and the minimum value is for ($\boldsymbol{TiO_2}$), due to it

containing lighter elements.

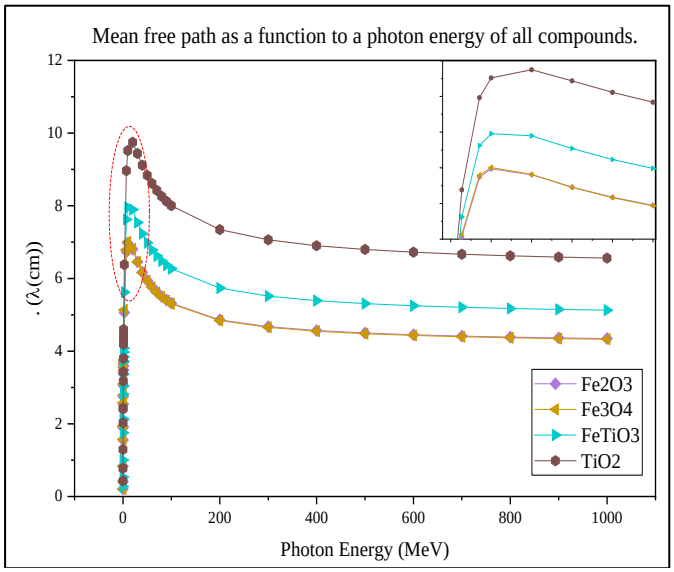

Fig (7): Electronic density versus photon energy.

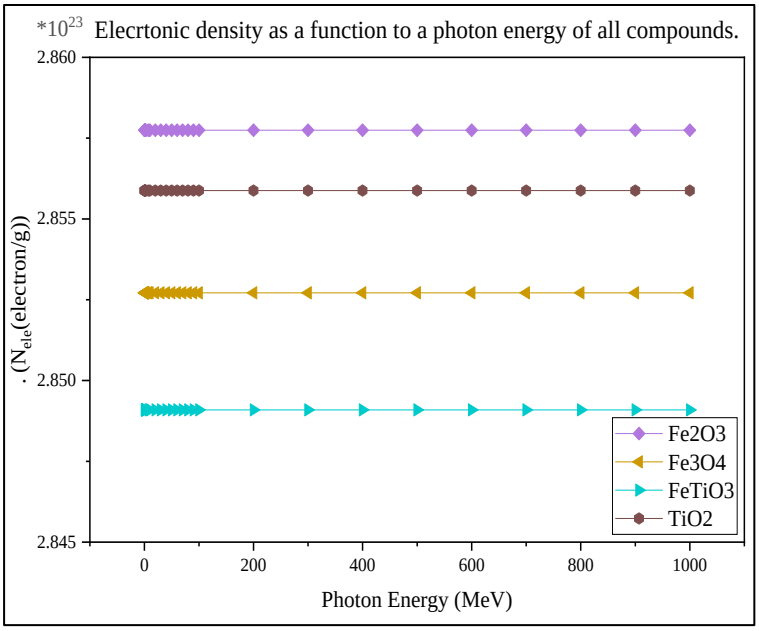

Fig (8): Mean free path versus photon energy.

Figure (7) shows the electronic density $\boldsymbol{N_e}$, since the quantity is related to $\boldsymbol{Z_{eff}}$, therefore its relationship with photons energy is constant, and is equal to $(\mathbf{2.85775, 2.85271, 2.84909, 2.85588}) \times \mathbf{10^{23}} \frac{\boldsymbol{e}}{\boldsymbol{g}}$ for $(\boldsymbol{Fe_2O_3, Fe_3O_4, FeTiO_3, TiO_2})$ compounds, respectively. The highest value was for $(\boldsymbol{Fe_2O_3})$, and the least value was for

($\boldsymbol{FeTiO_3}$) that because it's proportional to $\frac{\boldsymbol{\mu_t}}{\boldsymbol{\sigma_{t,e}}}$.

Figure (8) shows the mean free path λ, which starts small and increases rapidly as the photon energy increases until it reaches its highest value for the compound ($\boldsymbol{TiO_2}$), and then begins to decrease gradually and slowly when the phenomenon of pair production is the most common reaction, while the minimum value of $\boldsymbol{\lambda}$ is for the compound ($\boldsymbol{F3_3O_4}$) at the same energy, because the compound ($\boldsymbol{F3_3O_4}$) has a higher density and a greater effective atomic number than the compound ($\boldsymbol{TiO_2}$) which is lower in density and an effective atomic number.

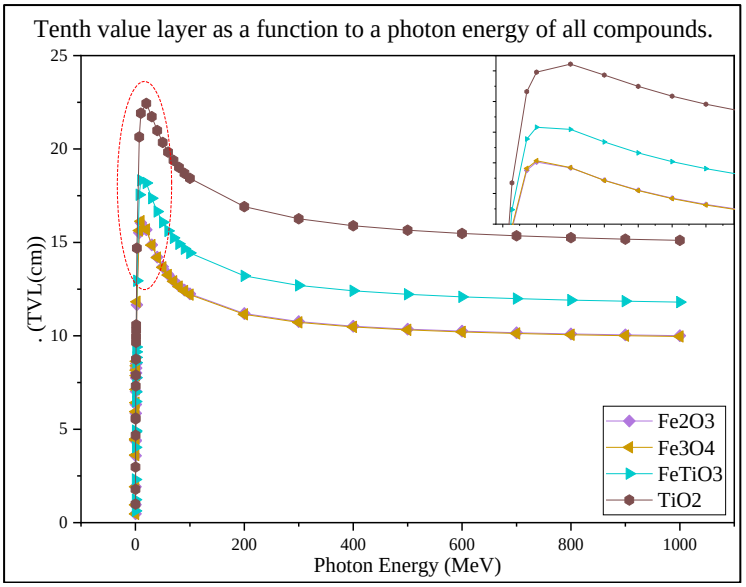

Fig (9): Half value layer versus photon energy.

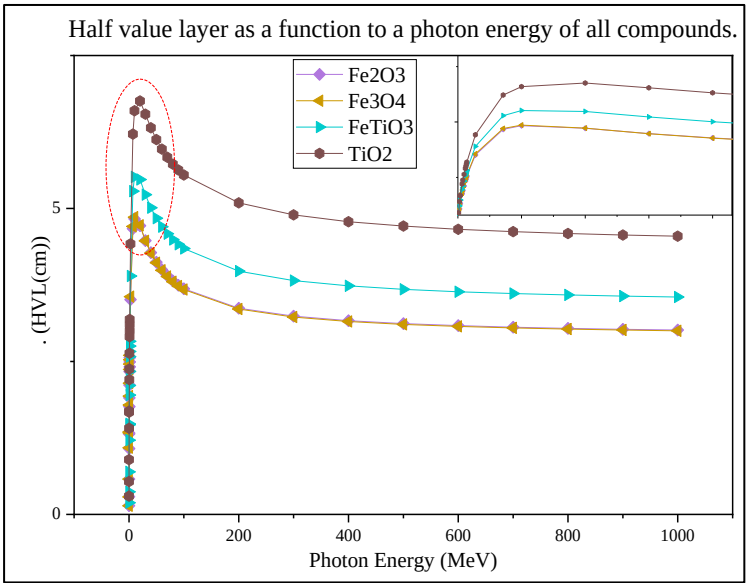

Fig (10): Tenth value layer versus photon energy.

Figures (9&10) show the half, tenth value layers (TVL & HVL), as they have small values at low energies, then they begin to increase when the photon energy increases, and they almost stabilize at high energies, that is, when the pair production reaction dominates. Their highest values are for the compound ($\boldsymbol{TiO_2}$), and their lowest value is for the compound ($\boldsymbol{F3_3O_4}$), this means high attenuation efficiency for this compound. The reason for the difference in values is due to the density of the two compounds and their containment of elements with different atomic numbers.

Table (2): shows the studied samples, their densities, concentrations [38].

Compounds	Samples	Concentration of TeO_2-B_2O_3%	$\rho\left(\frac{g}{cm^3}\right)$
$35TeO_2$-$50B_2O_3$-$5Bi_2O_3$-5BaO-5LiF	S1	35-50	4.13
$45TeO_2$-$40B_2O_3$-$5Bi_2O_3$-5BaO-5LiF	S2	45-40	4.53
$55TeO_2$-$30B_2O_3$-$5Bi_2O_3$-5BaO-5LiF	S3	55-30	4. 84
$65TeO_2$-$20B_2O_3$-$5Bi_2O_3$-5BaO-5LiF	S4	65-20	5.38
$75TeO_2$-$10B_2O_3$-$5Bi_2O_3$-5BaO-5LiF	S5	75-10	6.06

II- Neutrons attenuation - calculations

The (SAZ) program was used to calculate neutron attenuation parameters, which was written using the popular programming language Python version (3.10.11).

1- Neutrons attenuation - Glasses system attenuation

Some attenuation parameters have been calculated for the fast neutrons of the glass samples shown in table (2), which can be used in shielding processes in biological and medical applications, such as the formation of rays in neutron capture facilities with boron or lithium. Also, the low-energy gamma rays resulting from these captures can It is absorbed through this glassy material because it contains relatively heavy

metals. Balancing the components of this glass system can produce a highly efficient fast and thermal neutron absorber [38].

Table (3): Values of the parameters for fast neutrons using the SAZ code.

Compounds	$\boldsymbol{\Sigma_R}$ $(\boldsymbol{cm^{-1}})$ $(\boldsymbol{James})$	$\boldsymbol{\Sigma_R}$ $(\boldsymbol{cm^{-1}})$ [38]	$\boldsymbol{\lambda}$ $(\boldsymbol{cm})$ James	$\boldsymbol{\lambda}$ $(\boldsymbol{cm})$ [38]	HVL(cm) James	HVL(cm) [38]	TVL(cm) James	TVL(cm) [38]
S1	0.10910	0.10560	9.46969	9.16587	6.56389	6.35329	21.10519	21.80478
S2	0.11040	0.10731	9.31879	9.05766	6.45929	6.27829	20.85604	21.45732
S3	0.10933	0.10671	9.37119	9.14696	6.49562	6.34019	21.06164	21.57797
S4	0.11308	0.11085	9.02120	8.84344	6.25302	6.12980	20.36276	20.77208
S5	0.11894	0.11711	8.53898	8.40788	5.91877	5.82790	19.35987	19.66173

In table (3), $\boldsymbol{\Sigma_R}$ was calculated, and its largest and best value was for sample (S5) due to the large sample density compared to other samples, due to the large concentration of ($\boldsymbol{TeO_2}$) in the sample, and the result was in good agreement with [38], and $\boldsymbol{\Sigma_R}$ depends on the chemical content of the compound [2]. The lowest value was for the sample (S1), due to its relatively small mass density compared to the other sample [2].

Table (3) also shows the values of the mean free path $\boldsymbol{\lambda}$, and its least value is for the sample (S5) due to the inverse relationship between $\boldsymbol{\lambda}$ and $\boldsymbol{\Sigma_R}$, and due to the large density of the sample, and its highest value is for the sample (S1), due to its small mass density. We also note the great agreement of the results that obtained with [38].

Table (3) shows the values of the half and tenth value layers (TVL, HVL), as their highest values were for the sample (S1), and the lowest values were for the sample (S1) due to the inverse relationship between (TVL, HVL) and Σ_R, and this can be explained because the chemical content of the samples differed in their densities [38], and the results showed great agreement with [38].

2- Neutrons attenuation - Various samples

Table (4): Shows the values of shielding parameters for fast neutron using SAZ code and compares it with [8].

Samples / Parameters		Resin 250 WD	Dolomite sand	Aluminum Oxide	Steel Alloy
$\rho(g/cm^3)$		1.4	2.5	2.698	7.87
Σ_R	James	0.08248	0.09897	0.11494	0.16383
	Zoller	0.07677	0.09076	0.10494	0.15722
	[8]	0.11816	0.1011	0.13615	0.16937
λ (cm)	James	12.12356	10.10403	8.70049	6.10404
	Zoller	13.02627	11.0179	9.52907	6.36056
	[8]	8.46265	9.935206	7.34549	5.90419
HVL (cm)	James	8.40342	7.003579	6.03072	4.23100
	Zoller	9.02913	7.637026	6.60505	4.40880
	[8]	5.86586	6.88656	5.09150	4.09246
TVL (cm)	James	27.91554	23.26539	20.03363	14.05508
	Zoller	29.99410	25.36965	21.94150	14.64573
	[8]	19.48596	22.87666	16.91361	13.59491

Table (4) shows the values of the neutron attenuation parameters for the studied samples. The effective removal cross section Σ_R was calculated, and its biggest value was for (Steel Alloy), due to the high relative density of Fe in it compared to other samples, as it represents more

than 98% of the components of the alloy. Its smallest value was for the sample (Resin 250 WD) due to the low relative density of small elements in it. We also notice a good match between the results obtained with [8]. In fact, this means that maybe the SAZ code agrees with other programs such as (ParShield & MERCSG-N) in terms of the equations used, but it differs in terms of the programming language [8].

It also shows the values of the mean free path λ and compares them with [8], as its largest value was for the sample (Resin 250WD), due to the inverse proportionality between λ and Σ_R, and its lowest value was for the sample (Steel Alloy), which means that it is better in terms of attenuation. We also note from the results that λ with ρ for these samples is approximately the same, and the results obtained show a good agreement with [8].

Also, it shows the half, tenth values layers (HVL, TVL). We notice that they gradually decrease with increasing sample density. Their largest values were for the sample (Resin 250WD), while the lowest and best values were for the sample (Steel Alloy), and the results closely matched [8]. This means that it is preferable to use Steel Alloy as a shielding material against neutrons more than other samples because of its good shielding properties against neutrons.

Conclusions

In the current research, we studied the attenuation parameters against γ-rays for a group of compounds shown in table (1) based on NIST-XCOM database. The study showed that the compound (Fe_3O_4) has the best attenuation coefficients against γ-rays because it contains Iron with high ρ and Z. Neutron attenuation parameters were studied for samples of a glass system with different concentrations, in order to evaluate their ability to attenuate fast neutrons through a program that uses certain semi-empirical equations. Knowing the Σ_R values of the samples from the SAZ code, it became clear that the sample (S5) has the largest value among the glass samples, which agrees well with [38], which means that it is more suitable than other samples to be used in the design of shields in biological and medical applications that are used against neutrons. Other optional samples were also studied, shown in table (4), as the study showed that the Steel Alloy sample in the samples studied in [8] has better neutron attenuation parameters than the rest of the samples, because it has the largest value of Σ_R according to the semi-empirical equations, which are in good agreement with [8]. This means that it can be used as an attenuation shield against neutrons.

References

1. M.I. Sayyed, Shams A.M. Issa, Sayed H. Auda, Assessment of radio-protective properties of some anti-inflammatory drugs, Prog. Nucl. Energy 100 (2017) 297–308.
2. Elmahroug, Y., B. Tellili, and Ch Souga. "Calculation of fast neutron removal cross-sections for different shielding materials." International Journal of Physics and Research (IJPR) 3.2 (2013): 7-16.
3. Hubbell, J.H., 1999. Review of photon interaction cross section data in the medical and biological context. Phys. Med. Biol. 44, R1.
4. El-Khayatt, A. M. "NXcom–A program for calculating attenuation coefficients of fast neutrons and gamma-rays." Annals of nuclear energy 38.1 (2011): 128-132.
5. McAlister, Daniel R. "Gamma ray attenuation properties of common shielding materials." University Lane Lisle, USA (2012).
6. Al-Jaff, S. M. "Investigation the Effective atomic number, electron density, Half value layer and

mean free path of steel types 304 and 347 in the energy range (40-130) keV." Journal of Natural Sciences Research 5 (2013): 2225-0921.
7. Amanallah, Sabah Mahmoud, et al. "Calculation the Effective atomic number, electron density, half value layer and mean free path of Iron, Copper and Silver." Diyala Journal for Pure Science 10.3 (2014): 32-43.
8. Elmahroug, Y., et al. "ParShield: a computer program for calculating attenuation parameters of the gamma rays and the fast neutrons." Annals of Nuclear Energy 76 (2015): 94-99.
9. Biswas, Ripan, et al. "Calculation of gamma-ray attenuation parameters for locally developed shielding material: Polyboron." journal of radiation research and applied sciences 9.1 (2016): 26-34.
10. Zhou, Dong, et al. "Co-shielding of neutron and γ-ray with bismuth borate nanoparticles fabricated via a facile sol-gel method." Inorganic Chemistry Communications 77 (2017): 55-58.
11. Seenappa, L., et al. "Gamma, X-ray and neutron interaction parameters of Mg–Gd–Y–Zn–Zr alloys." Radiation Physics and Chemistry 150 (2018): 199-206.
12. Kaçal, M. R., F. Akman, and M. I. Sayyed. "Evaluation of gamma-ray and neutron attenuation properties of some polymers." Nuclear Engineering and Technology 51.3 (2019): 818-824.
13. Lakshminarayana, Gandham, et al. "Estimation of gamma-rays, and fast and the thermal neutrons attenuation characteristics for bismuth tellurite and bismuth boro-tellurite glass systems." Journal of Materials Science 55 (2020): 5750-5771.
14. Al-Tersawy, Sherif H., Rasha A. El-Sadany, and H. E. M. Sallam. "Experimental gamma-ray attenuation and theoretical optimization of barite concrete mixtures with nanomaterials against neutrons and gamma rays." Construction and Building Materials 289 (2021): 123190.
15. Sabry, N., et al. "Gamma-ray attenuation properties and fast neutron removal cross-section of Cu2CdSn3S8 and binary sulfide compounds (Cu/Cd/Sn S) using phy-X/PSD software." Radiation Physics and Chemistry 193 (2022): 109989.
16. Shamshon Somo Shlaimon, Sabah Mahmoud Amanallah, The shielding behavior of several hydrogenous materials for fast neutrons, Advances in mechanics, 11 2 (2023).
17. Shamshon Somo Shlaimon, Sabah Mahmoud Amanallah, Comparative study of neutrons shielding coefficients in different doped composite, Procedia of Theoretical and applied sciences, 11 sep (2023).
18. Robert E. Masterson, Nuclear Engineering Fundamentals, a Practical Perspective, Taylor & Francis Group, LLC, 2017.
19. N. M. Schaeffer, Reactor shielding for nuclear engineering, National Technical Information Service, 1973.
20. R. G. Jaeger. E. P. Blizard t, A. B. Chilton, M. Grotenhuis, A. Honig, Th. A. Jaeger H. H. Eisenlohr, Engineering Compendium on Radiation Shielding, Springer-Verlag Berlin Heidelberg 1968.
21. Burcu Akça and Salih Z. Erzeneoğlu, The Mass Attenuation Coefficients, Electronic, Atomic, and Molecular Cross Sections, Effective Atomic Numbers, and Electron Densities for Compounds of Some Biomedically Important Elements at 59.5 keV, Science and Technology of Nuclear Installations, Volume 2014, Article ID 901465.
22. Ravangvong, Sunantasak. "Calculation of fast neutron removal cross-sections for lithium borate glasses system doped lutetium." Journal of Materials Science and Applied Energy 9.1 (2020): 473-477.
23. D. F. Jackson and D. J. Hawkes, “X-ray attenuation coefficients of elements and mixtures,” Physics Reports, vol. 70, no. 3, pp. 169–233, 1981.
24. K. Singh and L. Gerward, “Summary of existing information on gamma-ray and X-ray attenuation coefficients of solutions,” Indian Journal of Pure and Applied Physics, vol. 40, no. 9, pp. 643–649, 2002.
25. Manohara, S. R., et al. "On the effective atomic number and electron density: a comprehensive

set of formulas for all types of materials and energies above 1 keV." Nuclear Instruments and Methods in Physics Research Section B: Beam Interactions with Materials and Atoms 266.18 (2008): 3906-3912.

26. S. R. Manohara, S. M. Hanagodimath, and L. Gerward, “Energy dependence of effective atomic numbers for photon energy absorption and photon interaction: studies of some biological molecules in the energy range 1 keV-20 MeV,” Medical Physics, vol. 35, no. 1, pp. 388–402, 2008.
27. Kavaz, E.; Tekin, H.; Agar, O.; Altunsoy, E.; Kilicoglu, O.; Kamislioglu, M.; Abuzaid, M.; Sayyed, M. The Mass stopping power/projected
28. Sayyed, M. I. "Half value layer, mean free path and exposure buildup factor for tellurite glasses with different oxide compositions." Journal of Alloys and Compounds 695 (2017): 3191-3197.
29. Alan Martin, Sam Harbison, Karen Beach, Peter Cole, An Introduction to Radiation Protection Seventh Edition, Taylor & Francis Group, LLC, 2019.
30. Thomas E. Johnson, Introduction to Health Physics, fifth edition, McGraw-Hill education, ISBN: 978-0-07-183526-8, 2017.
31. J. Wood, Computational methods in reactors shielding, (Pergamon press, New York, 1982).
32. J. Kenneth and E. Faw, fundamentals of nuclear science and engineering, New York: Marcel Dekker, 2002.
33. E. Abd, G. Mesbah, M. A. M. Nader and A. Ellithi, a simple method for determining the effective removal cross section for fast neutrons, Journal of Radiation and Nuclear Applications. 2(2) (2016) 53 – 58.
34. Al-Hadeethi, Y.; Sayyed, M.; Agar, O. Ionizing photons attenuation characterization of quaternary tellurite–zinc–niobium– gadolinium glasses using Phy-X/PSD software. J. Non-Cryst. Solids 2020, 538, 120044.
35. Sayyed, M., Kaky, K.M., ¸Sakar, E., Akbaba, U., Taki, M.M., Agar, O. Gamma radiation shielding investigations for selected germanate glasses. J. Non-Cryst. Solids 2019, 512, 33–40.
36. Heba Y. Zahran, El Sayed Yousef, Mohammed S. Alqahtani, Manuela Reben, Hamed Algarni, Ahmad Umar, Hasan B. Albargi, Ibrahim S. Yahia and Nehal Sabry, Analysis of the Radiation Attenuation Parameters of Cu2HgI4, Ag2HgI4, and (Cu/Ag/Hg I) Semiconductor Compounds, Crystals 2022, 12, 276.
37. Y. Elmahroug, B. Tellili, & C. Souga, Calculation of gamma and neutron shielding parameters for some materials Polyethylene - based removal cross-sections for different shielding materials, International Journal of Physics and Research (IJPR) ISSN 2250-0030 Vol. 3, Issue 2, Jun 2013, 7-16.
38. O. Olarinoye, Sultan Alomairy, Chahkrit Sriwunkum, H. H. Hegazy, M. S. Al-Buraihi, Effects of TeO2 and B2O3 on photon, neutron, and charged particle transmission properties of Bi2O3-BaO-LiF glass system, June, 2021, Journal of the Australian Ceramic Society 57 (14).